frontiers in Environmental Science

ORIGINAL RESEARCH
published: 09 March 2022
doi: 10.3389/fenvs.2022.857739

Coseismic Displacement and Slip Distribution of the 21 May 2021 Mw 6.1 Earthquake in Yangbi, China Derived From InSAR Observations

Yongsheng Li[1,2], Yujiang Li[1], Kuan Liang[1], Hao Li[1] and Wenliang Jiang[1]*

[1]National Institute of Natural Hazards, Ministry of Emergency Management of China, Beijing, China, [2]Key Laboratory of Landslide Risk Early-warning and Control, Ministry of Emergency Management of China, Chengdu, China

On 21 May 2021, a Mw 6.1 earthquake struck Yangbi County, Yunnan Province, China. In this study, InSAR data from Sentinel-1 SAR images were processed to image the coseismic deformation fields of the Yangbi earthquake. Then, the optimal slip model was obtained by applying the particle swarm optimization method. The interferometry results revealed that the earthquake triggered obvious surface deformation near the epicenter, while the earthquake did not produce an obvious surface rupture zone from field investigation. The optimal slip model suggests that the strike of the seismogenic fault responsible for this event is 139°, the dip angle is 81°, and the average rake angle is -170°. Additionally, the slip was concentrated mainly at depths of 2–8 km, the maximum dip-slip amount was 0.5 m, and the cumulative seismic moment reached 1.43×10^{18} N·m, equivalent to a Mw 6.1 earthquake. The geodetic and geophysical inversion results demonstrate that the Yangbi earthquake was dominated by a steeply dipping dextral strike-slip rupture. The rupture fault generally strikes NNW-SSE, which is consistent with that of the Weixi-Qiaohou fault, and may be a relatively new fault formed by an E-W-oriented extension of the western boundary of the Sichuan-Yunnan block. Finally, based on the InSAR results in combination with the spatial distribution characteristics of ground fissures and the strong historical earthquakes, we analyzed the tectonic background preceding the Yangbi earthquake and analyzed the relationship between the Yangbi earthquake and strong historical earthquakes in the region, thereby providing empirical evidence for analyzing seismic risk and fault rupture parameters, interpreting seismic deformation characteristics, and better understanding the seismogenic background of the western boundary of the Sichuan-Yunnan block.

Keywords: Yangbi Mw 6.1 earthquake, InSAR, slip distribution, focal mechanism inversion, stress change background

OPEN ACCESS

Edited by:
Chen Yu,
Newcastle University, United Kingdom

Reviewed by:
Lingyun Ji,
China Earthquake Administration, China
Chisheng Wang,
Shenzhen University, China
Wu Zhu,
Chang'an University, China

****Correspondence:***
Yujiang Li
yujiangli@ninhm.ac.cn

Specialty section:
This article was submitted to Environmental Informatics and Remote Sensing, a section of the journal Frontiers in Environmental Science

Received: *19 January 2022*
Accepted: *11 February 2022*
Published: *09 March 2022*

Citation:
Li Y, Li Y, Liang K, Li H and Jiang W (2022) Coseismic Displacement and Slip Distribution of the 21 May 2021 Mw 6.1 Earthquake in Yangbi, China Derived From InSAR Observations. Front. Environ. Sci. 10:857739. doi: 10.3389/fenvs.2022.857739

INTRODUCTION

According to the China Seismic Network, on 21 May 2021, a Mw 6.1 earthquake struck Yangbi County, Yunnan Province, at (25.67°E, 99.87°N), the depth of hypocenters was 8 km (Li C. et al., 2021; Hu et al., 2021). Different research institutions have provided focal mechanism solutions for this earthquake using the global or regional network data (**Table 1**). This earthquake is generally characterized as a dextral strike-slip event (Liu et al., 2021). Based on the earthquake epicenter, this event occurred along the western boundary of the Sichuan–Yunnan block, which is consistent with the movement properties and

TABLE 1 | Focal mechanisms and fault parameters from different studies.

Source	Epicenter		Focal mechanisms	Mag (Mw/Ms)	Depth (km)	References
	Lon (°E)	Lat (°N)				
Regional seismic network	99.87	25.67	138°/82°/-161°	Mw 6.0	5	http://www.cea-igp.ac.cn/kydt/278248.html
P-wave	99.87	25.67	141°/68°/-153°	Ms 6.4	-	http://www.cea-igp.ac.cn/kydt/278248.html
Far-field body wave	100.008	25.67	135°/82°/-	Mw6.1	11	http://www.cea-igp.ac.cn/kydt/278248.html
USGS	100.016	25.744	135°/82°/-165°	Mw 6.1	9	https://earthquake.usgs.gov/earthquakes/eventpage/us7000e532/executive
InSAR	99.934	25.644	139°/81°/-170°	Mw 6.1	6	Yang Z. et al., 2021
InSAR	99.87	25.67	316°/86°/-	Mw 6.14	3–13	Zhang K. et al., 2021
InSAR	99.93	25.64	139°/81°/-171°	Mw 6.1	6	This Study

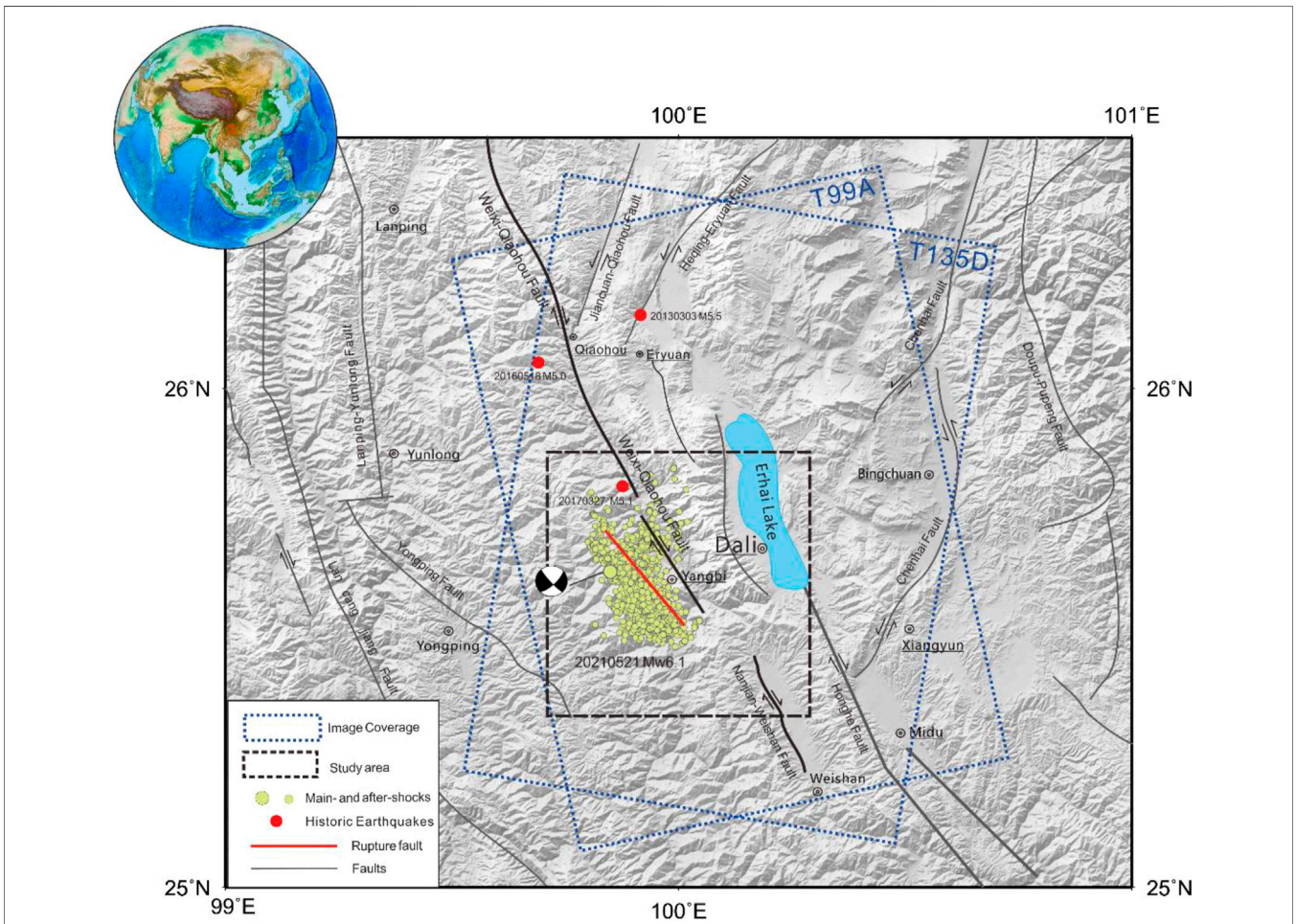

FIGURE 1 | Active faults and seismotectonic background of the region surrounding the Yangbi earthquake. The China Earthquake Networks Center provided the locations of historical earthquakes. The yellow dots denote the Yangbi Mw 6.1 mainshock and aftershock (Su et al., 2021).

trends of the Red River and Weixi–Qiaohou fault zones (**Figure 1**), the latter of which has been characterized by dextral strike-slip movement since the late Quaternary (Chang et al., 2016a; Zhang K. et al., 2021). There are no obvious surface ruptures that have been found in field investigations. Consequently, the identity and geometric characteristics of the seismogenic fault responsible for the Yangbi earthquake need to be further clarified. In particular, intensive research must be conducted to ascertain whether the Weixi–Qiaohou fault zone, which represents the closest fault to the epicenter of the Yangbi event or an unknown hidden fault, was responsible for this earthquake, and the characteristics of such a hidden fault must be thoroughly investigated.

In recent years, earth observation technologies such as interferometric synthetic aperture radar (InSAR) have been

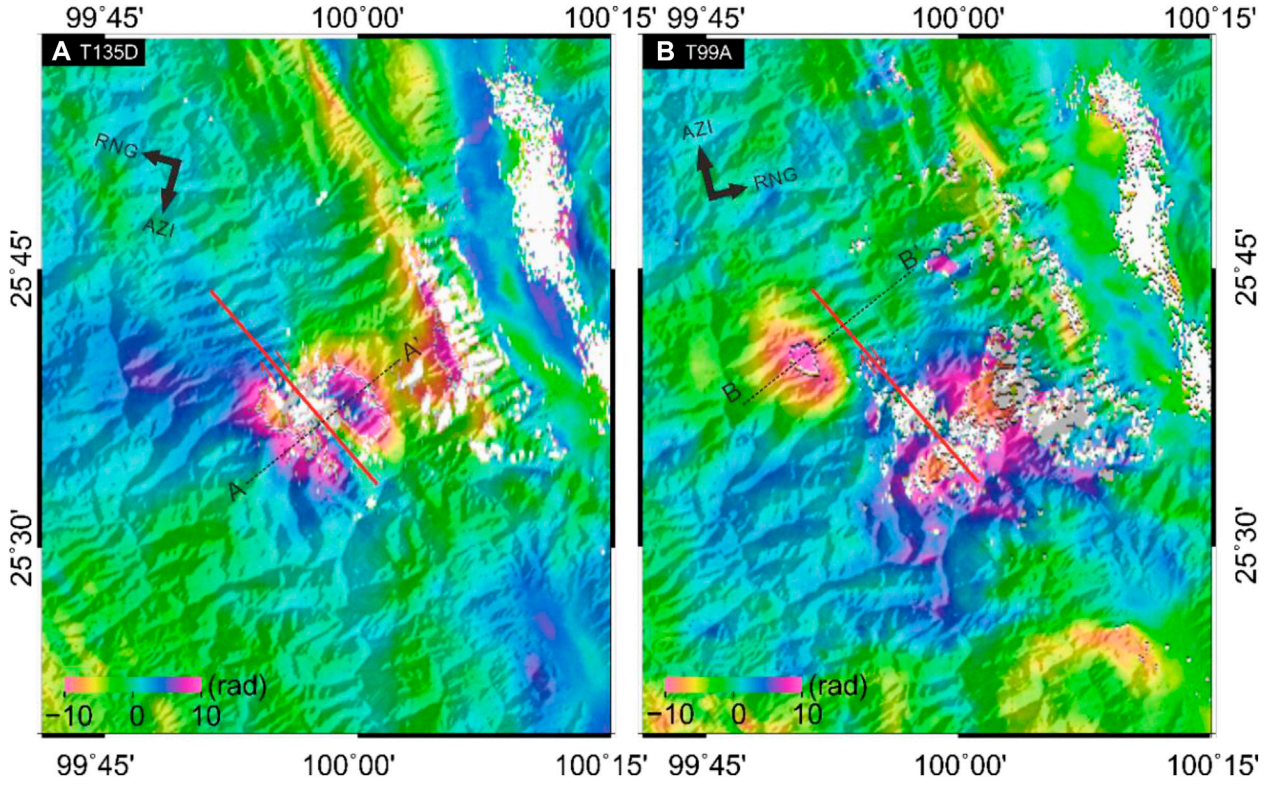

FIGURE 2 | (A) Coseismic deformation fields of the Yangbi earthquake are calculated from Sentinel-1 descending track 163. **(B)** Coseismic deformation fields calculated from ascending track 99. The red line represents the inferred ruptured fault, and the black dotted lines indicate the cross-sections perpendicular to the inferred fault.

employed to remotely monitor the Earth's surface to quantify global surface microdeformation globally with high precision (Li et al., 2020; Li K. et al., 2021; Li B. et al., 2020). In this paper, the InSAR coseismic deformation fields of the Yangbi earthquake were mapped using Sentinel-1 images acquired in terrain observation with progressive scans (TOPS) mode, and the focal mechanism and fault slip distribution were calculated and discussed. Analyzing the focal mechanism of the Yangbi Mw6.1 earthquake has essential theoretical and practical significance for fundamentally understanding the seismotectonic background, the structural deformation mechanism, and the activities along the block boundary in NW Yunnan. In particular, studying the seismotectonic activity in this region is crucial to understanding the tectonic background of the southeastern Qinghai–Tibet Plateau.

TECTONIC SETTING

The Yangbi earthquake occurred along the southwestern boundary of the rhombic Sichuan–Yunnan block (**Figure 1**), which has been forming since the early Cenozoic as a result of the eastward extrusion of the Qinghai–Tibet Plateau. During this time, the southeastward motion of the Sichuan–Yunnan block resulted in the development of a series of active right-lateral, oblique NW-trending faults in this region, obstructed by the South China block. The Sichuan–Yunnan block shifted toward the SE and rotated clockwise around the East Himalayan tectonic junction. Consequently, the Sichuan–Yunnan block is the most representative active block (featuring the strongest lateral extrusion) along the eastern margin of the Qinghai–Tibet Plateau (Long et al., 2021) and, being a research hotspot for studying the movement and tectonic deformation of rigid blocks, is the focus of many investigations on active tectonics and earthquake monitoring and prediction (Chang et al., 2016b). The northeastern and eastern boundaries of the Sichuan-Yunnan block are controlled by the Ganzi-Yushu, Xianshuihe-Anninghe-Zemuhe, and Xiaojiang fault segments and other fault zones, all of which are characterized by sinistral strike-slip and high slip rates. In particular, the eastern boundary of this block has a clear structure and frequently experiences earthquakes (Ren et al., 2007).

The Yangbi earthquake occurred in an active fault zone traversing the western boundary of the Sichuan-Yunnan block and is where the Weixi-Qiaohou-Weishan fault connects with the Red River fault, both of which are NW-trending dextral strike-slip faults. The main well-known active segments are situated near the epicenter of the 2021 Yangbi event. As major faults, the Weixi-Qiaohou-Weishan fault and Red River fault control the crustal deformation along the southwestern boundary of the Sichuan-Yunnan block (Wang S. et al., 2021). Using the cut-and-paste (CAP) waveform inversion method (Wang Y. et al., 2021a), the epicenter of the Yangbi

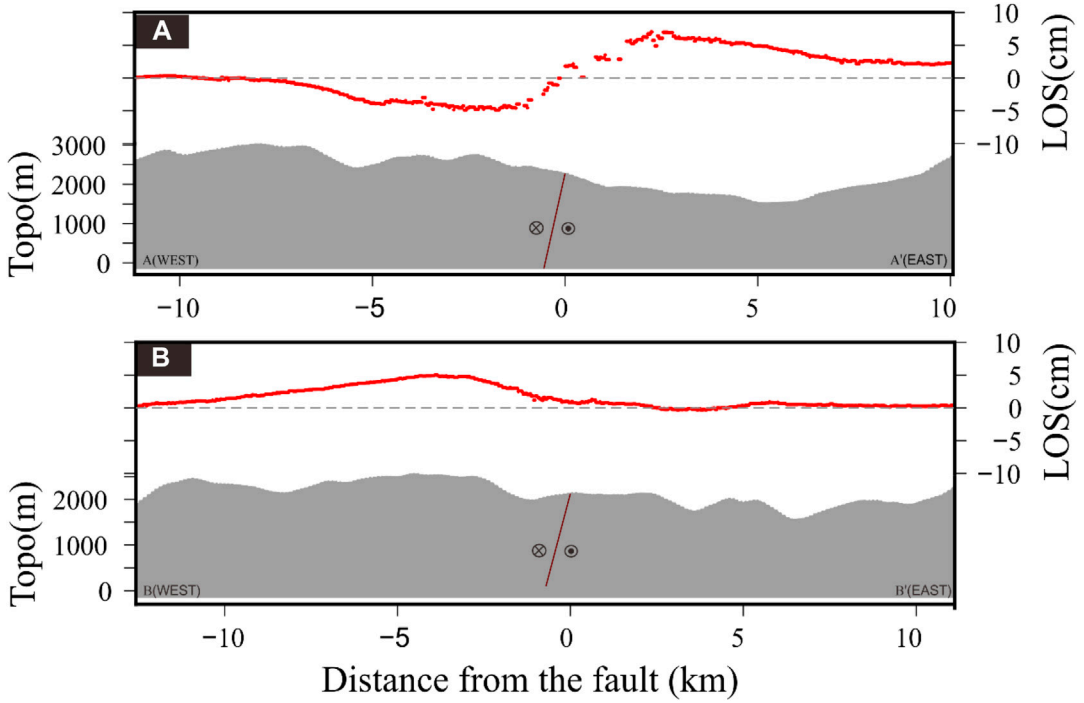

FIGURE 3 | (A) Profile of the coseismic LOS deformation along line A-A′ in Figure 2A. **(B)** Profile of the coseismic LOS deformation changes along line B-B′ in **Figure 2B**.

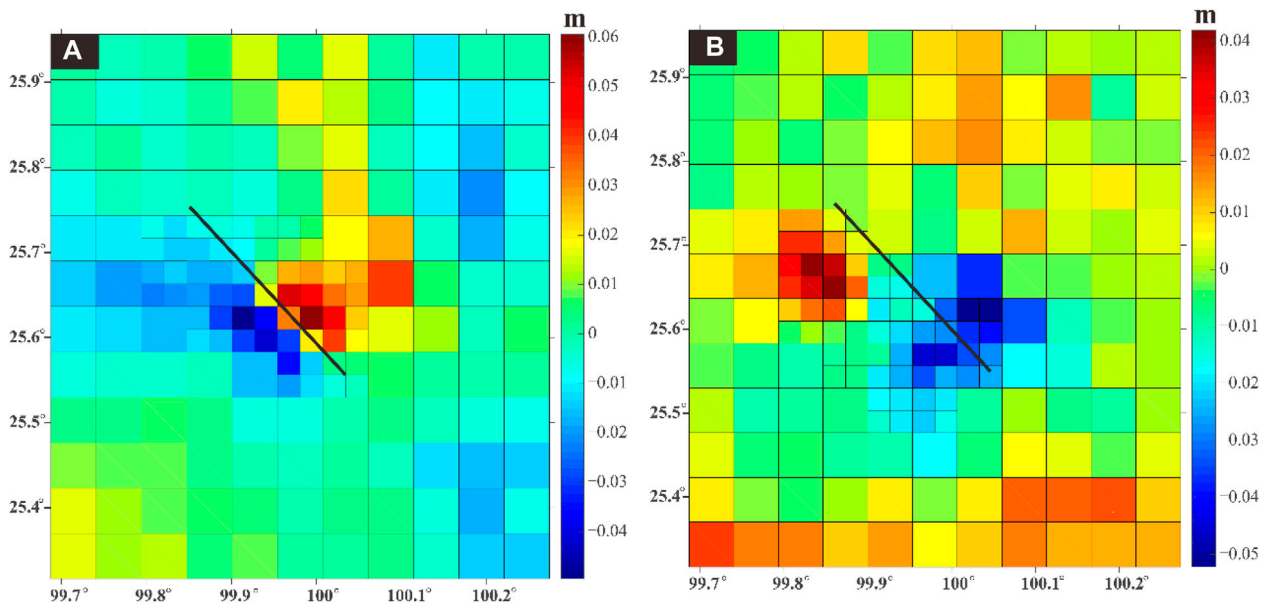

FIGURE 4 | Quadtree downsampling results of the coseismic deformation fields corresponding to **(A)** descending track 163 in Figure 2A and **(B)** ascending track 99 in Figure 2B.

earthquake sequence was shown to be approximately 3–10 km SW along the Weixi–Qiaohou fault and the long axis of the aftershock area was reported to trend NW–SE.

The Weixi–Qiaohou fault is a large-scale boundary fault that starts in northwestern Weixi County and connects with the Red River fault in southern Weishan, spanning approximately 280 km

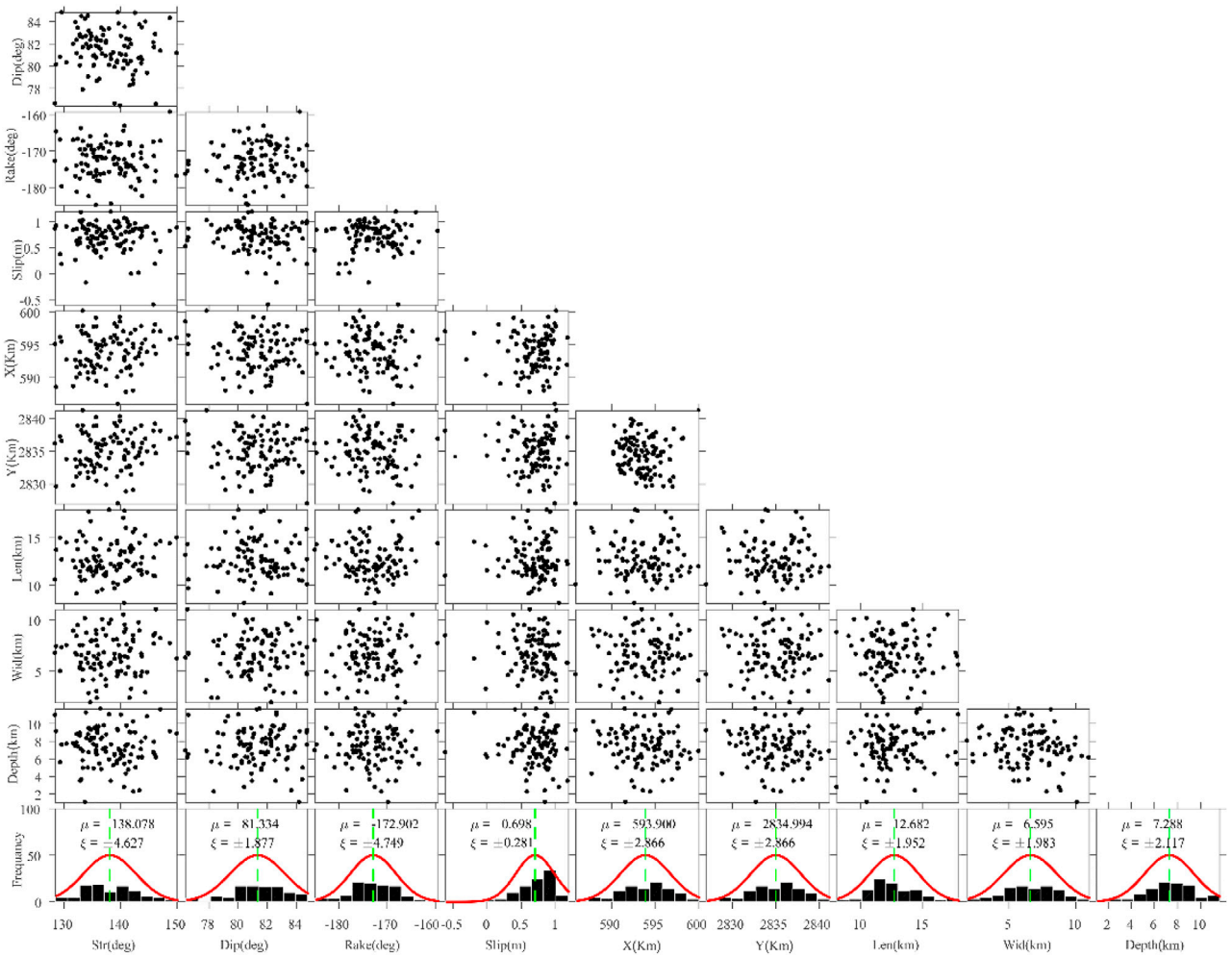

FIGURE 5 | Uncertainties and trade-offs for the nonlinear inversion computed using Monte Carlo analysis.

with a general strike of NNW–SSE (**Figure 1**). The fault shows strong late Quaternary activity, which has manifested in new active landforms such as straight fault troughs, clear fault triangles, and fault scarps (Ren et al., 2007; Duan et al., 2021). The fault is dominated by dextral strike-slip with a minor normal slip component, and ridges and water systems show apparent synchronous dextral dislocations along the fault (Li D. et al., 2021). Because the historical records of earthquakes in this region are not noteworthy, this area has received little attention for many years. However, many moderately strong earthquakes have recently occurred, such as the 2017 Yangbi Ms5.1 earthquake (25 km from the epicenter of the 2021 Yangbi Mw6.1 earthquake), the 2016 Yunlong Ms5.0 earthquake (59 km from the epicenter), and the 2013 Eryuan Ms5.5 earthquake (31 km away from the epicenter) (**Figure 1**). These phenomena suggest that the tectonic activity in this region is gradually increasing.

INSAR COSEISMIC DEFORMATION

The focal mechanisms and waveform inversion results reported by previous studies show that the seismogenic fault that produced the Yangbi earthquake exhibited dextral strike-slip motion (Ye et al., 2021; Yang Z. et al., 2021). However, the overall deformation amplitude is small from field investigation, and there are almost no signs of rupture on the surface. To image the coseismic deformation field generated by this earthquake, the Sentinel-1 satellite equipped with C-band SAR launched by the European Space Agency was employed in this paper. Sentinel-1 descending track 135 and ascending track 99 data with interferometric wide swath (IW) mode were obtained (**Figure 1**). Using an automatic seismic deformation monitoring system for Sentinel-1 SAR data (Li Y. et al., 2021), the ascending and descending InSAR coseismic deformation fields were obtained, as shown in **Figure 2**. The Advanced

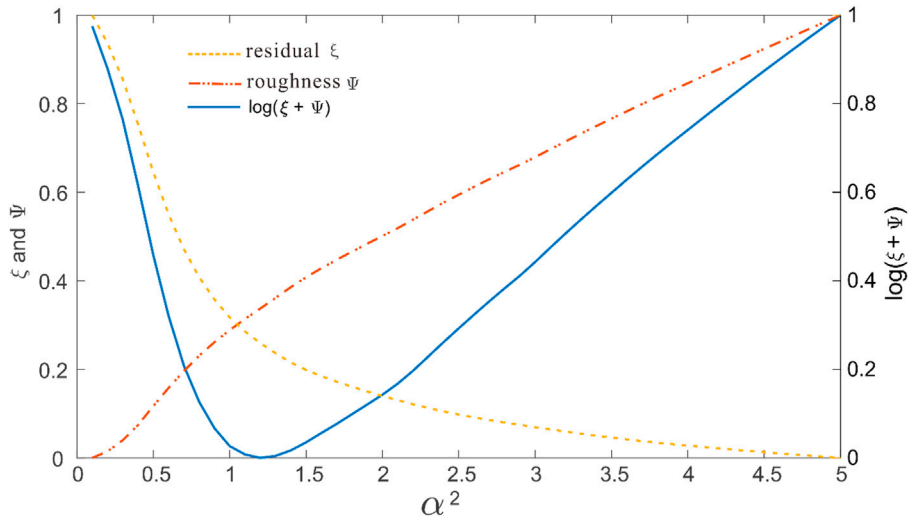

FIGURE 6 | Trade-off curves line the residuals (ξ) and roughness (ψ). The solid line represents the normalized log ($\psi + \xi$).

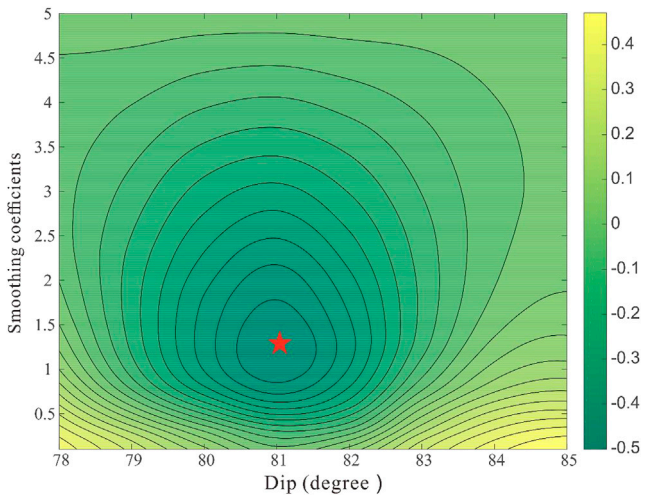

FIGURE 7 | Contour map of the log function with variations in the dip and smoothing coefficients (α2). The red star indicates the global minimum.

Land Observing Satellite Global Digital Surface Model (ALOS World 3D) with a 30-m resolution was used as external digital elevation model (DEM) data to eliminate the phase contribution of undulating terrain (Tadono et al., 2014). Additionally, an adaptive Goldstein filtering algorithm was applied to filter the original interferograms (Goldstein et al., 1988), and the minimum cost flow algorithm was used for phase unwrapping (Chen and Zebker, 2000). The atmospheric delay error was preliminarily corrected by the Generic Atmospheric Correction Online Service for InSAR (GACOS) method (Yu et al., 2018), and the residual orbit was fitted by linear fitting.

The resulting coseismic deformation field based on Sentinel-1 satellite data can clearly describe the spatial distribution and magnitude of deformation caused by the Yangbi earthquake (**Figure 2**). The results predominantly indicate that the strike of the fault is NNW–SSE, which is consistent with recent aftershock location findings (Su et al., 2021). After correcting the atmospheric contribution, the coseismic interferogram of the descending track in **Figure 2A** reflects a clear deformation pattern. The long axis is distributed in the NW–SE direction. There are obvious deformation signals distributed on both sides of the inferred fault (the surface to the SW of the fault is moving away from the satellite, while that to the NE is moving toward the satellite). Cross sections perpendicular to the inferred fault were selected to conduct a profile analysis (**Figure 3A**), revealing that the maximum deformation in the line-of-sight (LOS) direction on the NE side reached approximately 8 cm, while that on the SW side was approximately 5 cm. The ascending coseismic interferogram (**Figure 2B**) shows an obvious deformation pattern moving toward the satellite in the epicenter area, reaching 5 cm in the LOS direction (**Figure 3B**). However, the deformation field cannot accurately describe the coseismic deformation characteristics of this strike-slip earthquake, mainly because the azimuth of the ascending track is nearly consistent with the fault strike. Therefore, the SAR sensor is not sensitive enough to capture the deformation signal parallel to the surface movement direction.

FOCAL MECHANISM INVERSION

After unwrapping the InSAR interferograms, the data were downsampled using the quadtree method constrained by the data resolution (Lohman and Simons 2005; Feng et al., 2018; 2019). The large deformation gradients in the downsampled interferograms are mainly in the areas with large surface deformation, while the deformation gradients are low in the far field (**Figure 4**). This downsampled measurement ensures the inversion accuracy and dramatically reduces the

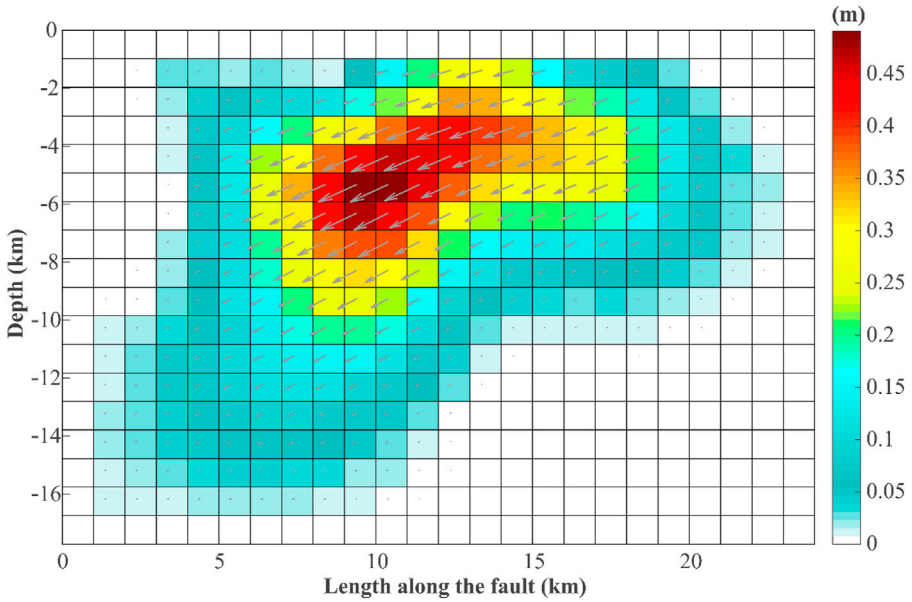

FIGURE 8 | Optimal slip distribution of the Yangbi earthquake. The gray arrows represent the hanging wall's motion direction relative to the footwall.

computational cost of the inversion. Then, the downsampled deformation fields were employed as inversion constraints, and the geometric parameters and slip distribution of the fault were estimated by a two-step inversion method (Feng et al., 2013). The fault parameters and slip mechanism of the Yangbi earthquake were studied as described below.

Uniform Slip

We assumed a uniform slip model to determine the fault's geometric parameters of the fault, including epicenter location (latitude/longitude), strike, dip, and top and bottom depths. Then, the rupture slip distribution on the rectangular fault plane was estimated by a nonlinear inversion algorithm (Feng et al., 2013; Li B. et al., 2020; Yang J. et al., 2021). We used the Particle Swarm Optimization and okada inversion package (PSOKINV) (Feng et al., 2013) to ensure that the source parameters could be successfully retrieved under relatively few parameter constraints. The adaptive function is defined as

$$\sigma = \sqrt{\frac{(W(D - GS))^2}{N}}, \quad (1)$$

where G is Green's function, with the coefficient matrix representing the surface motion in response to 1 m of dip-slip on a uniform fault, S is the slip vector at each patch, W is the weight matrix, D is the observed surface deformation, and N is the number of observed deformations (Feng et al., 2013).

To evaluate the reliability of the nonlinear inversion of source parameters, we added Gaussian-distributed error to the original observations to generate 100 perturbed datasets. Then, we performed a Monte Carlo test to estimate the uncertainties and trade-offs for the geometric parameters during the nonlinear inversion (Parsons et al., 2006). The test results (Fig. 5) revealed that the uncertainties are small and that the trade-offs are strong enough to indicate that the nonlinear inversion estimates are reliable.

The nonlinear inversion results suggest that the major seismogenic fault is a dextral strike-slip fault with a strike of ~139°, a dip of ~81°, and an average rake angle of approximately -173°. Moreover, the optimal inverted slip model suggests that coseismic slip was concentrated at a depth of 7.2 km with a maximum slip of ~0.7 m.

Distributed Slip

We then conducted a linear inversion to estimate the slip distribution during the Yangbi earthquake and fixed the optimal geometry of the fault plane determined from the uniform slip solution. The fault plane was extended to 24 km long and 18 km wide, and the size of each slip patch was set to 1 km × 1 km. To prevent physically impossible oscillatory slip and determine the optimal fitting solution, we applied a log function $f(\delta, a^2) = \log(\psi + \xi)$ to find the optimal dip angle and smoothing factor for the distributed slip model. ξ and ψ represent the residual and slip roughness, respectively, and a^2 and δ represent the smoothing factor and dip angle, respectively (Burgmann et al., 2002). According to the literature, the above log function can effectively determine the optimal dip and smoothness coefficient simultaneously (Feng et al., 2013).

With normalization, the residual curve is a monotonically decreasing function, while the roughness is a monotonically increasing function. The optimal smoothing factor was determined to be $a^2 \approx 1.2$ (**Figure 6**). We set the dip angle in the range of [78°, 85°] and the smoothing factor in the domain of [0.1 5] and then iterated the dip angle and smoothing factor to perform an additional grid search for the optimal dip. The

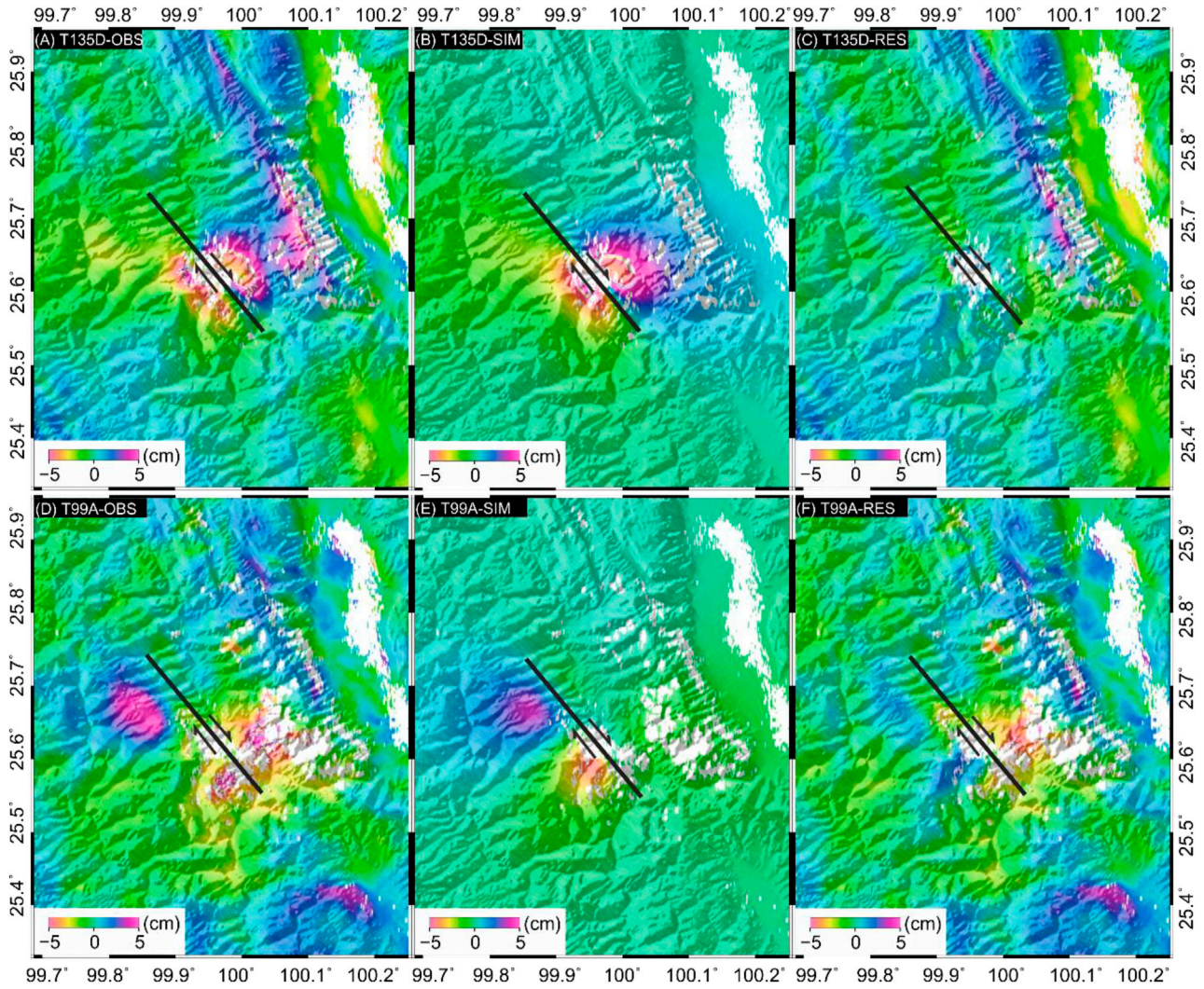

FIGURE 9 | (A) and **(D)** Observed coseismic deformation fields for descending track 135 and ascending track 99, respectively. **(B)** and **(E)** Corresponding simulated deformation. **(C)** and **(F)** Corresponding residuals. Positive values represent movement toward the satellite, while negative values represent movement away from the satellite.

optimal dip angle and smoothing coefficients were determined by obtaining global minima of 81° and 1.2, respectively (**Figure 7**).

Finally, we obtained the best-fitting slip model shown in **Figure 8**, suggesting that this event ruptured on a dextral strike-slip fault with a strike of ~139°, a dip of ~81°, and an average rake angle of -170°. A slip was concentrated mainly at depths of 2–8 km and spanned a distance of 20 km. The maximum amount of slip reached 0.5 m at a depth of 6 km, and the corresponding moment magnitude was Mw 6.1. **Figure 9** represents the observed displacements, simulated results derived from the optimal slip model, and residuals between the observation and simulation. Our distributed slip model can sufficiently explain the general deformation pattern from both tracks. There are no notable residual fringes except for some contributions from the atmospheric disturbance in the far field (**Figures 9C,F**), which suggest that the inversion results are stable and reliable.

DISCUSSION

Verification of the Field Investigation Results

Seismic activity produces ground fissures due to either shear or tensile stresses that alter the stress state of rock and soil masses near the Earth's surface (Li C. et al., 2021). To accurately map and quantitatively measure the surface rupture associated with the Yangbi earthquake, we carried out a field investigation around the epicenter of this event. No obvious surface rupture was found, but we discovered that many fresh cracks had formed during the earthquake. By measuring the trends of

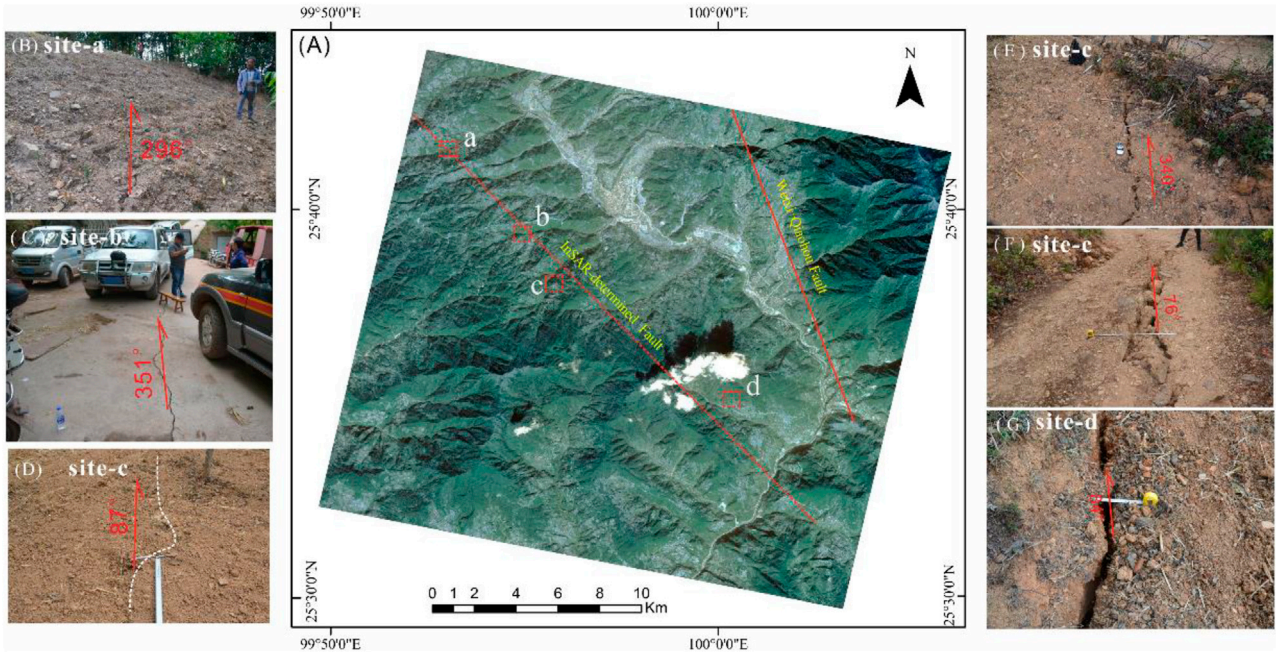

FIGURE 10 | Remote sensing images of the epicenter of the Yangbi earthquake and its on-site photos of ground fissures. **(A)** Optical image of the earthquake epicenter acquired on 19 November 2020, by the Gaofen-2 sensor, The red dotted line indicates the estimated fault of this event. The solid red line represents the Weixi-Qiao fault **(B)** Field photo of the ground fissure at point a, **(C)** reveals point b **(D)**, **(E)**, **(F)** represent point c, and **(G)** indicates point d.

these fissures in the field, we determined that these fissures trend mostly NW–SE, and the fissures show the characteristics of dextral strike-slip. The spatial distribution of crack locations illustrates that the fissured area is roughly distributed in a NW–SE strip that is completely consistent with the fault determined from InSAR (**Figure 10**). These ground fissures have obvious directionality, and their strikes are consistent with that of the rupturing fault. Therefore, we infer that their locations are controlled by the fault. We selected several representative points for analysis. At points a and b in **Figure 10A**, the spatial orientations of the ground fissures are basically consistent with those of the inferred fault (**Figures 10B,C**). In contrast, those of the ground fissures at points c and d are disordered, with the ground fissures distributed in all directions (**Figures 10D–G**). We stipulate that this irregular distribution results from slope and terrain influences. There are no obvious surface cracks near the Weixi–Qiaohou fault, which has a low earthquake intensity. Therefore, the field investigation further verified that the seismogenic structure of the earthquake was a new NW-trending blind fault.

Rupture Structure and Seismogenic Mechanism

The Weixi–Qiaohou, Red River, Jinshajiang, and Deqin–Zhongdian–Daju faults constitute the western boundary of the active Sichuan–Yunnan block. They, therefore, play essential roles in the formation, evolution, and movement of the block (Li et al., 2021). Specifically, the southwestern boundary of the Sichuan–Yunnan block exhibits a high strike-slip rate in response to the lateral extrusion of crustal material from the Qinghai–Tibet Plateau. The boundary of the block is not a single fault but rather a group of dispersed and complex dextral strike-slip faults (Long et al., 2021). The evolutionary history of these faults reflects mutual structural transformation, stress generation, and strain weakening between them. The tectonic interactions, stresses, and deformation among these faults may constitute the main mechanism of absorbing the eastward extrusion of the Qinghai–Tibet Plateau. In this process, some fault activities weaken, and new faults arise with the expansion of existing major faults.

The fault location determined by InSAR and the spatial distribution of relocated aftershocks show that the seismogenic fault of the Yangbi earthquake is far from known active faults and is approximately 4–10 km from the nearest segment of the Weixi–Qiaohou–Weishan fault zone (Fig. 11). According to the characteristics of coseismic deformation, the seismogenic segment belongs to a branch fault at the junction between the Weixi–Qiaohou–Weishan fault and Red River fault zones and may be a secondary fault of the Weixi–Qiaohou–Weishan fault (Chang et al., 2016b; Yang J. et al., 2021). The seismogenic fault is associated with and parallel to the Weixi–Qiaohou fault. The formation of this structure may be related to the southeastward motion of the Sichuan–Yunnan block and the clockwise rotation in SW Yunnan (Fig. 11). The clockwise rotation in SW Yunnan exerts a drag force on the SW wall of the NW-SE-trending

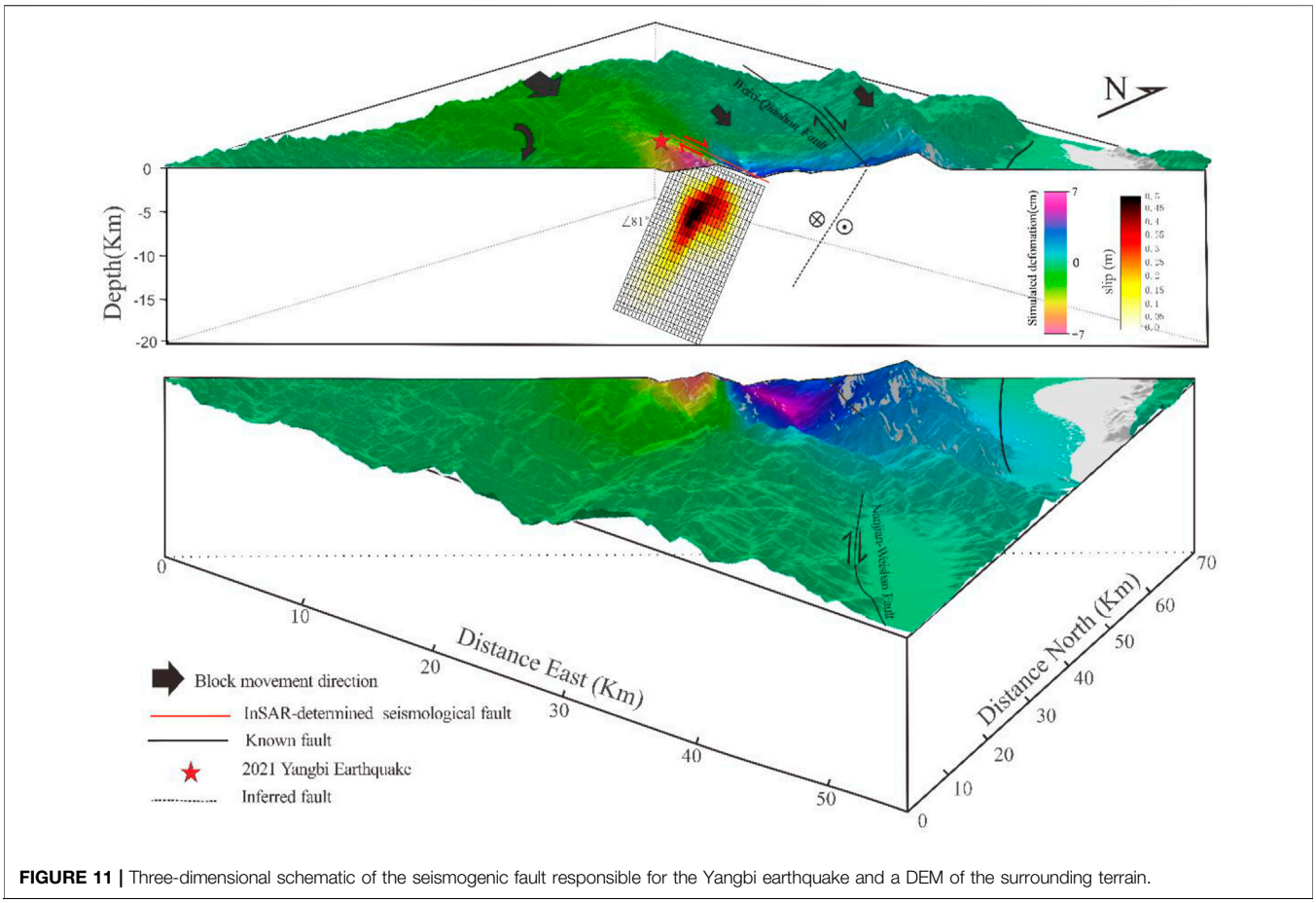

FIGURE 11 | Three-dimensional schematic of the seismogenic fault responsible for the Yangbi earthquake and a DEM of the surrounding terrain.

seismogenic fault. This may be the main dynamic cause of this quake event. In addition, the EW extension results in the dip component of the fault (Chang et al., 2016a; Long et al., 2021).

Stress Change Background of Earthquake Occurrence

The Yangbi event was a strong earthquake that occurred on a secondary fault in the Sichuan–Yunnan block. The characteristics of the regional stress field are critical to understanding its seismogenic mechanism. Thus, the focal mechanism solutions of 27 strong historical earthquakes (Mw > 6.5) in this region (Li et al., 2020; Zhang et al., 1989) were utilized to estimate the stress tensor (Gephart and Forsyth, 1984; Wan, 2015), and then we obtained the three principal stress directions and stress shape factors on a 0.1°×0.1° grid (Angelier, 1979).

Using the optimal stress tensor obtained from the method of Li et al. (2020), the potential rupture plane of future strong earthquakes in the region was determined (**Figure 12**). The NW–SE-trending seismogenic faults in the vicinity of the Yangbi earthquake epicenter are characterized by dextral strike-slip, which is consistent with the InSAR inversion results (139°/81°/-170°), the focal mechanism parameters derived from seismological data (Long Y. et al., 2021; Wang Y. et al., 2021b), and the fault motion characteristics implied by the

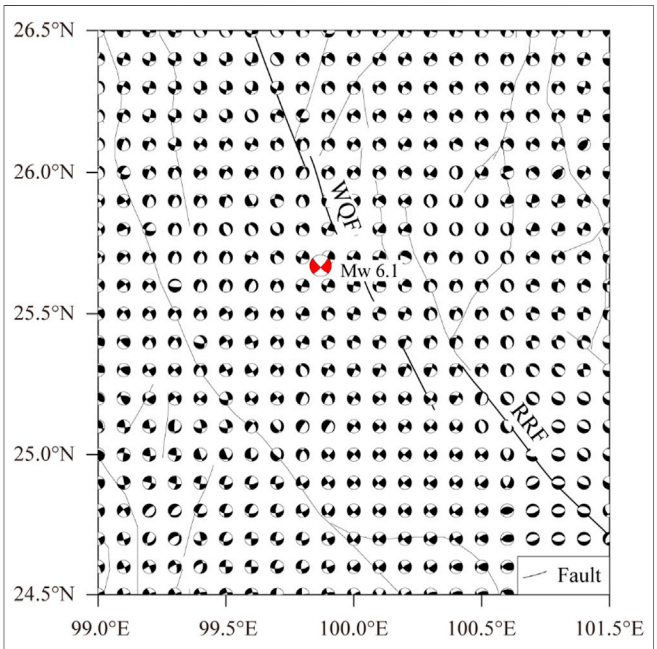

FIGURE 12 | The potential rupture plane of future strong earthquakes in the region is determined based on historical earthquake focal mechanisms (WQF: Weixi-Qiaohou fault; RRF: Red River fault).

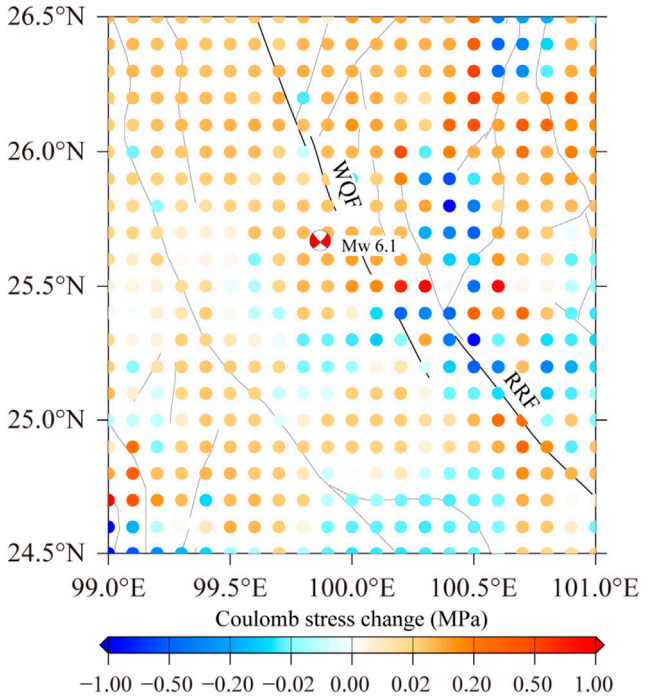

FIGURE 13 | Coulomb stress changes in the area surrounding the Yangbi earthquake epicenter and potential rupture planes caused by strong historical earthquakes (WQF: Weixi–Qiaohou fault; RRF: Red River fault).

focal mechanisms of aftershocks (Zhang et al., 2022). The direction of the maximum principal compressive stress and principal compressive strain in the region is NNW–SSE (Hu et al., 2017; Wang and Shen, 2020), which can effectively explain the seismogenesis of the Yangbi earthquake and the earthquakes in the surrounding area dominated by dextral strike-slip.

Since the occurrence of the Yangbi earthquake, many studies have focused on the impact of the earthquake on the future seismic risk of the surrounding faults (Yang Z. et al., 2021; Zhang B. et al., 2021), although few studies have addressed the possible relationship between the Yangbi earthquake and strong historical earthquakes in the region. Based on the potential rupture planes of future strong earthquakes shown in **Figure 13**, the optimal and auxiliary rupture planes were used as the receiving fault for a stress tensor projection. The maximum Coulomb stress was selected to represent the stress change at the source (Toda and Enescu, 2011) to analyze the changes in the Coulomb stress on the seismogenic fault caused by strong historical earthquakes. The historical earthquake source model and medium model are referred to Li Y. et al. (2020). According to the resulting Coulomb stress changes (**Figure 12**), strong historical earthquakes produced an obvious stress increase at the epicenter of the Yangbi earthquake, and the stress increment exceeded the stress trigger threshold of 0.1 bar, which promoted the occurrence of the Yangbi earthquake. In addition, we found the northwestern RRF is also within the influence scope of positive Coulomb stress changes, which inferred that the northwestern RRF is an area requiring special attention.

CONCLUSION

In this study, the coseismic deformation field produced by the Yangbi earthquake that occurred on 21 May 2021, was derived from Sentinel-1 ascending and descending track data. Taking the deformation fields as constraints, a two-step inversion strategy was applied to estimate the geometric structure and slip distribution of the rupture plane. The PSOKINV method was employed to find the best solution that minimizes the fitting function in the whole parameter domain. The inferred optimal slip model suggests that the rupture surface of the earthquake trends NNW–SSE and is predominantly a steeply dipping dextral strike-slip fault. This reveals that the coseismic slip distribution was controlled by secondary faults west of the Weixi–Qiaohou fault. The earthquake nucleated at a shallow depth on the rupture plane, and the major seismogenic fault was a dextral strike-slip fault with a strike of ~139°, a dip of ~81° to the southwest, and an average rake angle of -170°. A maximum slip of ~0.5 m was achieved at a depth of 6 km. The cumulative seismic moment reached up to 1.43×10^{18} N·m, equivalent to a magnitude of Mw 6.1. According to the resulting Coulomb stress changes, the strong historical earthquakes produced an obvious stress increase at the epicenter of the Yangbi earthquake and promoted the occurrence of the Yangbi earthquake. The efficient and accurate analysis of the focal mechanism of the Yangbi earthquake is of great significance for interpreting coseismic deformation characteristics and facilitating the rapid deployment of earthquake emergency rescue personnel. Moreover, this work is expected to benefit further research on the geological structure and kinematic mechanism of the Weixi–Qiaohou fault and the active prediction of geological disasters.

DATA AVAILABILITY STATEMENT

The original contributions presented in the study are included in the article/Supplementary Material, further inquiries can be directed to the corresponding author.

AUTHOR CONTRIBUTIONS

YL contributed to the conception of the study, performed the experiment and writen YL contributed to the conception of the study, performed the data analyses and wrote the manuscript KL performed the field inverestment and analyses HL contributed significantly to analysis and manuscript preparation WJ helped perform the analysis with constructive discussions.

FUNDING

This research is partly supported by research grants from the National Institute of Natural Hazards, MEMC (grant

numbers No. ZDJ 2019-17); the National Natural Science Foundation of China (no. 41704051,41772219); National Key Research and Development Program of China (2021YFC3001903) and Gaofen earthquake monitoring and emergency application demonstration (phase II) (31_Y30F09-9001-20/22).

REFERENCES

Angelier, J. (1979). Determination of the Mean Principal Directions of Stresses for a Given Fault Population. *Tectonophysics* 56, T17–T26. doi:10.1016/0040-1951(79)90081-7

Burgmann, R., Ayhan, M. E., Fielding, E. J., Wright, T. J., McClusky, S., Aktug, B., et al. (2002). Deformation during the 12 November 1999 Duzce, Turkey, Earthquake, from GPS and InSAR Data. *Bull. Seismological Soc. America* 92, 161–171. doi:10.1785/0120000834

Chang, Z., Chang, H., and Dai, B. (2016b). Recent Active Features of Weixi-Qiaohou Fault and its Relationship with the Honghe Fault. *Journal geomechanics* 22 (3), 517

Chang, Z., Chang, H., Li, J., Dai, B., Zhou, Q., Zhu, J., et al. (2016a). The Characteristic of Active Normal Faulting of the Southern Segment of Weixi-Qiaohou Fault. *Joural Seismological Res.* 39 (4).

Chen, C. W., and Zebker, H. A. (2000). Network Approaches to Two-Dimensional Phase Unwrapping: Intractability and Two New Algorithms. *J. Opt. Soc. Am. A.* 17 (3), 401–414. doi:10.1364/josaa.17.000401

Duan, M., Zhao, C., Zhou, L., Zhao, C., and Zuo, K. (2021). Seismogenic Structure of the May 21 2021 MS6.4 Yunnan Yangbi Earthquake Sequence. *Chin. J. Geophys.* 64 (9), 3111–3125. doi:10.6038/cjg2021P0423

Feng, W., Li, Z., Elliott, J. R., Fukushima, Y., Hoey, T., Singleton, A., et al. (2013). The 2011 MW 6.8 Burma Earthquake: Fault Constraints provided by Multiple SAR Techniques. *Geophys. J. Int.* 195, 650–660. doi:10.1093/gji/ggt254

Feng, W., Samsonov, S., Almeida, R., Yassaghi, A., Li, J., Qiu, Q., et al. (2018). Geodetic Constraints of the 2017 M W 7.3 Sarpol Zahab, Iran Earthquake, and its Implications on the Structure and Mechanics of the Northwest Zagros Thrust-Fold Belt. *Geophys. Res. Lett.* 45 (14), 6853–6861. doi:10.1029/2018gl078577

Feng, W., Samsonov, S., Liang, C., Li, J., Charbonneau, F., Yu, C., et al. (2019). Source Parameters of the 2017Mw 6.2 Yukon Earthquake Doublet Inferred from Coseismic GPS and ALOS-2 Deformation Measurements. *Geophys. J. Int.* 216 (3), 1517–1528. doi:10.1093/gji/ggy497

Gephart, J. W., and Forsyth, D. W. (1984). An Improved Method for Determining the Regional Stress Tensor Using Earthquake Focal Mechanism Data: Application to the San Fernando Earthquake Sequence. *J. Geophys. Res.* 89, 9305–9320. doi:10.1029/jb089ib11p09305

Goldstein, R. M., Zebker, H. A., and Werner, C. L. (1988). Satellite Radar Interferometry: Two-Dimensional Phase Unwrapping. *Radio Sci.* 23 (4), 713–720. doi:10.1029/RS023i004p00713

Hu, J., Zhao, T., Bai, C., Guo, H., Wang, Y., Li, X., et al. (2021). Three-dimensional P and S Wave Velocity Structure and Earthquake Relocation of the May 21, 2021 Yangbi MS6.4 Source Region. *Chin. J. Geophys.* 64 (12), 4488–4509. doi:10.6038/cjg2021P0456

Hu, X., Zang, A., Heidbach, O., Cui, X., Xie, F., and Chen, J. (2017). Crustal Stress Pattern in China and its Adjacent Areas. *J. Asian Earth Sci.* 149, 20–28. doi:10.1016/j.jseaes.2017.07.005

Li, B., Li, Y., Jiang, W., Su, Z., and Shen, W. (2020). Conjugate Ruptures and Seismotectonic Implications of the 2019 mindanao Earthquake Sequence Inferred from Sentinel-1 InSAR Data. *Int. J. Appl. Earth Observation Geoinformation* 90, 102127. doi:10.1016/j.jag.2020.102127

Li, Y., Shi, F. Q., Zhang, H., Wei, W. X., Xu, J., and Shao, Z. G. (2020). Coulomb Stress Change on Active Faults in Sichuan-Yunnan Region and its Implications for Seismic hazard. *Seismol. Geol.* 42, 526

Li, C., Zhang, J., Wang, W., Sun, K., and Shan, X. (2021). The Seismogenic Fault of the 2021 Yunnan Yangbi Ms6.4 Earthquake. *Seismology Geology.* 43 (3), 706

Li, D., Ding, Z., Wu, P., Liu, S., Deng, P., Liu, S., et al. (2021). The Characteristics of Crustal Structure and Seismogenic Background of Yangbi MS6.4 Earthquake on May 21, 2021 in Yunnan Province, China. *Chin. J. Geophys.* 64 (9), 3083–3100. doi:10.6038/cjg2021P0405

Li, K., Li, Y., Tapponnier, P., Xu, X., Li, D., and He, Z. (2021). Joint InSAR and Field Constraints on Faulting during the Mw 6.4, July 23, 2020, Nima/Rongma Earthquake in central Tibet. *J. Geophys. Res. Solid Earth* 126, e2021JB022212. doi:10.1029/2021jb022212

Li, Y., Jiang, W., Zhang, J., Li, B., Yan, R., and Wang, X. (2021). Sentinel-1 SAR-Based Coseismic Deformation Monitoring Service for Rapid Geodetic Imaging of Global Earthquakes. *Nat. Hazards Res.* 1 (1), 11–19. doi:10.1016/j.nhres.2020.12.001

Liu, J., Gan, W., Wang, G., Wang, Z., Zhang, Y., and Cai, H., L. (2021). Seismic Moment Tensor and Seismogenic Structure of the Yangbi MS6.4 Earthquake Sequence on May 21, 2021 in Yunnan. *Chin. J. Geophys.* 64 (12), 4475–4487. doi:10.6038/cjg2021P0559

Lohman, R. B., and Simons, M. (2005). Some Thoughts on the Use of InSAR Data to Constrain Models of Surface Deformation: Noise Structure and Data Downsampling. *Geochem. Geophys. Geosyst.* 6, a–n. doi:10.1029/2004GC000841

Long, F., Qi, Y. P., Yi, G. X., Wu, W. W., Wang, G. M., Zhao, X. Y., et al. (2021). Relocation of the Ms 6.4 Yangbi Earthquake Sequence on May 21, 2021 in Yunnan Province and its Seismogenic Structure Analysis. *Chin. J. Geophys.* 64, 263

Parsons, B., Wright, T., Rowe, P., Andrews, J., Jackson, J., Walker, R., et al. (2006). The 1994 Sefidabeh (Eastern Iran) Earthquakes Revisited: New Evidence from Satellite Radar Interferometry and Carbonate Dating about the Growth of an Active Fold above a Blind Thrust Fault. *Geophys. J. Int.* 164, 202–217. doi:10.1111/j.1365-246x.2005.02655.x

Ren, J., Zhang, S., Hou, Z., and Liu, X. (2007). Study of Late Quaternary Slip Rate in the Mid-segment of the Tongdian-Weishan Fault. *Seismology Geology.* 29 (4), 756

Su, J., Liu, M., Zhang, Y., Wang, W., Li, H., Yang, J., et al. (2021). High Resolution Earthquake Catalog Building for the May 21 2021 Yangbi, Yunnan, MS6.4 Earthquake Sequence Using Deep-Learning Phase Picker. *Chin. J. Geophys* 64 (8), 2647–2656. doi:10.6038/cjg2021O0530

Tadono, T., Ishida, H., Oda, F., Naito, S., Minakawa, K., and Iwamoto, H. (2014). Precise Global DEM Generation by ALOS PRISM. *ISPRS Ann. Photogramm. Remote Sens. Spat. Inf. Sci.* II-4, 71–76. doi:10.5194/isprsannals-ii-4-71-2014

Toda, S., and Enescu, B. (2011). Rate/state Coulomb Stress Transfer Model for the CSEP Japan Seismicity Forecast. *Earth Planet. Sp* 63, 171–185. doi:10.5047/eps.2011.01.004

Wan, Y. G. (2015). A Grid Search Method for Determination of Tectonic Stress Tensor Using Qualitative and Quantitative Data of Active Faults and its Application to the Urumqi Area. *Chin. J. Geophys.* 58, 3144

Wang, M., and Shen, Z.-K. (2020). Present-Day Crustal Deformation of Continental China Derived from GPS and its Tectonic Implications. *J. Geophys. Res.* 125, e2019JB018774. doi:10.1029/2019jb018774

Wang, S., Liu, Y., and Shan, X. (2021). Coseismic Surface Deformation and Slip Models of the 2021 Ms6.4 Yangbi (Yunnan, China) Earthquake. *Seismology Geology.* 43 (3), 692

Wang, Y., Chen, K., Shi, Y., Zhang, X., Chen, S., Li, P. e., et al. (2021b). Source Model and Simulated Strong Ground Motion of the 2021 Yangbi, China Shallow Earthquake Constrained by InSAR Observations. *Remote Sensing* 13, 4138. doi:10.3390/rs13204138

Wang, Y., Hu, S., He, X., Guo, K., Xie, M., Deng, S., et al. (2021a). Relocation and Focal Mechanism Solutions of the May 21 2021 MS6.4 Yunnan Yangbi Earthquake Sequence. *Chin. J. Geophys.* 64 (12), 4510–4525. doi:10.6038/cjg2021P0401

Yang, J., Wen, Y., and Xu, C. (2021). The May 21 2021 MS6.4 Yangbi (Yunnan) Earthquake: A Shallow Strike-Slip Event Rupturing in a Blind Fault. *Chin. J. Geophys.* 64 (9), 3101–3110. doi:10.6038/cjg2021P0408

Yang, Z., Liu, J., Liu, J., Zhang, X.-M., Deng, W., Du, G., et al. (2021). A Preliminary Report of the Yangbi, Yunnan, MS6.4 Earthquake of May 21, 2021. *Earth Planet. Phys.* 5 (4), 1–3. doi:10.26464/epp2021036

Ye, T., Chen, X., Huang, Q., and Cui, T. (2021). Three-dimensional Electrical Resistivity Structure in Focal Area of the Yangbi Ms6.4 Earthquake and its Possible Seismogenic Mechanism. *Chin. J. geophys.* 64 (7), 2267–2276. doi:10.6038/cjg2021O0523

Yu, C., Li, Z., Penna, N. T., and Crippa, P. (2018). Generic Atmospheric Correction Model for Interferometric Synthetic Aperture Radar Observations. *J. Geophys. Res. Solid Earth* 123 (10), 9202–9222. doi:10.1029/2017jb015305

Zhang, C., Cao, X., and Qu, K. (1989). *Earthquake Focal Mechanism in China*. Beijing: Academic Books Press.

Zhang, Y., An, Y., Long, F., Zhu, G., Qin, M., Zhong, Y., et al. (2022). Short-Term Foreshock and Aftershock Patterns of the 2021 Ms 6.4 Yangbi Earthquake Sequence. *Seismological Soc. America* 93, 21–32. doi:10.1785/0220210154

Zhang, B., Xu, G., Lu, Z., He, Y., Peng, M., and Feng, X. (2021). Coseismic Deformation Mechanisms of the 2021 Ms 6.4 Yangbi Earthquake, Yunnan Province, Using InSAR Observations. *Remote Sensing* 13, 3961. doi:10.3390/rs13193961

Zhang, K., Gan, W., Liang, S., Xiao, G., Dai, C., Wang, Y., et al. (2021). Coseismic Displacement and Slip Distribution of the 2021 May 21, Ms6.4, Yangbi Earthquake Derived from GNSS Observation. *Chin. J. geophys.* 64 (7), 2053–2266. doi:10.6038/cjg2021O0524

Conflict of Interest: The authors declare that the research was conducted in the absence of any commercial or financial relationships that could be construed as a potential conflict of interest.

Publisher's Note: All claims expressed in this article are solely those of the authors and do not necessarily represent those of their affiliated organizations, or those of the publisher, the editors, and the reviewers. Any product that may be evaluated in this article, or claim that may be made by its manufacturer, is not guaranteed or endorsed by the publisher.

Copyright © 2022 Li, Li, Liang, Li and Jiang. This is an open-access article distributed under the terms of the Creative Commons Attribution License (CC BY). The use, distribution or reproduction in other forums is permitted, provided the original author(s) and the copyright owner(s) are credited and that the original publication in this journal is cited, in accordance with accepted academic practice. No use, distribution or reproduction is permitted which does not comply with these terms.